

Modelling Creep in Toughened Epoxy Adhesives

This Electronic Guide was produced as part of the Measurements for Materials System Programme on Design for Fatigue and Creep in Joined Systems

[Introduction](#)

[Materials](#)

[Creep Model for Toughened Adhesives](#)

[Implementation of the Creep Model in a Finite Element Analysis](#)

[FEA of a Lap Joint Specimen](#)

[Observations regarding Long-Term Failure](#)

[Further Reading](#)

[Full contents page is available](#)

Introduction

Previous studies on adhesives at NPL have shown how finite element analysis can be used to predict extensions in an adhesively bonded joint that is under an applied load, as well as distributions of stress and strain within the adhesive layer. The purpose behind these studies has been to improve the use of finite element analysis as a tool for designing bonded joints. The results of an analysis can be used to explore variations in the design of the joint in order to reduce stress or strain levels in regions of stress concentration.

In conjunction with a valid failure criterion, it should be possible to predict the ultimate load that the joint can sustain. Confidence in predictions requires the use of models that accurately describe the deformation behaviour of the adhesive as well as accurate property data for the adhesive. Emphasis has therefore been given in earlier studies to the evaluation of models in finite element packages for describing the non-linear and strain-rate-dependent deformation behaviour of toughened adhesives. Test methods were also developed for characterising deformation behaviour and for determining the properties and parameters required by the models.

This work has demonstrated that the mechanical properties of adhesives vary with strain rate or time under load as expected for viscoelastic materials. This means that under long-term loading, properties will decrease progressively with time, and stress and strain levels in the adhesive will be very different from predictions based on a short-term analysis under monotonic loading. In addition, criteria for failure of the adhesive or parameters in these criteria will probably depend upon factors such as the load history and the time under load.

In order for a stress analysis to assist with the design of bonded joints in these situations, models are needed that describe deformation of the adhesive under creep, intermittent or fatigue loads. The work reported here is the first stage of such a programme. It considers deformation and failure under a long-term load of constant magnitude (creep). Measurements and modelling have been carried out of the creep behaviour of two toughened epoxy adhesives. The onset of non-linear behaviour in creep tests is observed at somewhat lower stresses than obtained in previous work in short-term tests under monotonic loading. The non-linearity arises because of a progressive reduction, with stress level, in the relaxation times of the molecular relaxation processes associated with the creep deformation. The reduction in relaxation times is related to the stress state as well as the stress magnitude.

This behaviour cannot be modelled using available non-linear creep models in finite element packages so a new model has been developed. An attempt has been made to implement this with the solver in Abaqus through the preparation of a user-defined subroutine for application with a generalised model in ABAQUS for time-dependent plasticity. This has enabled changes in distributions of stress and strain in the adhesive in a lap joint to be calculated with time under load. These results are compared with approximate values calculated using long-term, isochronous data with an elastic-plastic materials model.

Materials

Creep studies have been carried out on two rubber-toughened epoxy adhesives. Standard tensile specimens were cut from the sheets for the measurement of creep behaviour under uniaxial tensile stress. Sheets of bulk resin with a thickness of approximately 3 mm were cast in a mould.

XD 4601

- One-part adhesive supplied by Dow Plastics.
- Cured at a temperature of 180 °C for 1 hour.

DP460

- Two-part system supplied by 3M Ltd.
- Left for 24 hours at a temperature of 23 °C and subsequently post-cured at 100 °C for 30 minutes.

[Home](#) | [Introduction](#) | [Materials](#) | [Creep model](#) | [Implementation in Abaqus](#) | [FEA of a lapjoint](#) | [Failure](#) | [Further reading](#)

Creep Model for Toughened Adhesives

[Linear Creep](#)

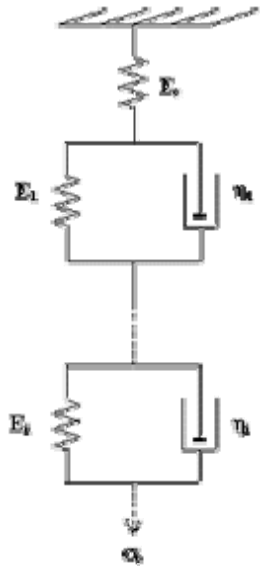
[Physical Ageing](#)

[Non-Linear Creep](#)

[Creep under Multiaxial Stress States](#)

Linear Creep

Spring and Dashpot



The time-dependent, viscoelastic behaviour of polymeric materials may be modelled with combinations of spring and viscous dashpot elements in series and parallel.

For a model consisting of the 3 elements E_0 , E_1 and η_1 , the strain response $\epsilon(t)$ to a constant stress σ_0 is

$$\epsilon(t) = \frac{\sigma_0}{E_0} + \frac{\sigma_0}{E_1} \left(1 - \exp - \left(\frac{t}{\tau_1} \right) \right) \quad (1a)$$

where the relaxation time τ_1 is given by

$$\tau_1 = \frac{\eta_1}{E_1} \quad (1b)$$

This single relaxation time model will not describe actual relaxation processes in polymers, which have a very broad distribution of relaxation times. The model can be extended, through the incorporation of additional spring and dashpot (Voigt) elements in series to broaden the spectrum of relaxation times and hence the time span of the relaxation process being modelled.

The strain response now to an applied stress is

$$\epsilon(t) = \frac{\sigma_0}{E_0} + \sigma_0 \sum_{i=1}^n \frac{1}{E_i} \left(1 - \exp - \left(\frac{t}{\tau_i} \right) \right) \quad (1c)$$

where there are n Voigt elements in the model.

The large number of parameters that need to be determined in this model is inconvenient and is usually not necessary for modelling creep in glassy polymers at temperatures well below the glass-to-rubber transition temperature.

Simplest model that shows both a short-term, elastic or unrelaxed response as well as a long-term, limiting deformation corresponding to a fully relaxed state.

Empirical Relationships for Creep Compliance

From the spring and dashpot model the strain response to an applied stress is

$$\varepsilon(t) = \frac{\sigma_o}{E_o} + \sigma_o \sum_{i=1}^n \frac{1}{E_i} \left(1 - \exp - \left(\frac{t}{\tau_i} \right) \right) \quad (2a)$$

Creep strains can be described by a simpler expression

$$\varepsilon(t) = \frac{\sigma_o}{E_o} \exp \left(\frac{t}{t_o} \right)^m \quad (2b)$$

This function will only model the short-time tail of the relaxation function given by Equation (2a), but this is usually a valid approximation, even for extended periods under load, as long as the measurement temperature is not close to the glass transition temperature. In Equation (2b), the exponent m characterises a broad spectrum of relaxation times whose mean or effective value is t_o .

Equation (2b) can also be expressed as a creep compliance function $D(t)$ where

$$D(t) = \frac{\varepsilon(t)}{\sigma_o} = D_o \exp \left(\frac{t}{t_o} \right)^m \quad (2c)$$

The magnitude of the parameter t_o depends on

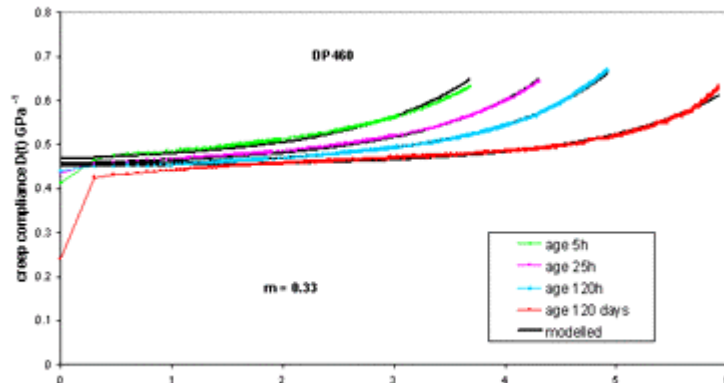
- temperature
- stress level. The dependence on stress level gives rise to [non-linear creep](#) behaviour
- stress state , such as a [multiaxial stress state](#)
- state of [physical ageing](#) of the adhesive at the time of the creep loading

Physical Ageing

Physical ageing in glassy polymers occurs after the polymer is cooled to temperatures below the rubber-to-glass transition.

At an elevated temperature, where a polymer is in the rubbery state, the structure of the material, as determined by molecular conformations, is in equilibrium. As the temperature is cooled through the glass transition temperature, conformational changes that are needed to maintain an equilibrium structure are restricted by the increase in the relaxation times (reduced mobility) of molecular rearrangements at the lower temperatures. These non-equilibrium structures have a relatively high mobility to relaxation processes under creep loading, and this gives rise to relatively rapid creep at short elapsed times after cooling. Despite the low temperature of the glassy polymer, there is sufficient molecular mobility for structural changes to take place with subsequent elapsed time (physical ageing) leading to structural states that become progressively closer to equilibrium for the low temperature.

These ageing processes give rise to a reduction in molecular mobility under creep and a shift in creep curves to longer creep times as observed in the figure below. This figure shows experimental data for the creep compliance of the adhesive DP460 with time under a stress of $\sigma_0 = 6.6$ MPa at different states of physical ageing. The age state is determined by the elapsed time t_e after cooling from the post-cure temperature of 100 °C.



The creep behaviour can be modelled using the creep compliance function $D(t)$:

$$D(t) = \frac{\varepsilon(t)}{\sigma_0} = D_0 \exp\left(\frac{t}{t_0}\right)^m \quad (3a)$$

The continuous lines are best fits to data at each elapsed time. The only parameter to change in each curve is the mean relaxation time t_0 .

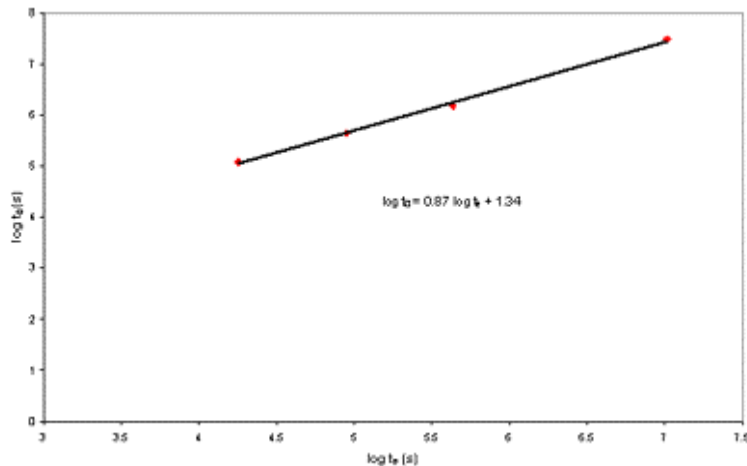
[Physical Ageing continued.....](#)

Creep compliance curves for DP460 at a stress $\sigma_0 = 6.6$ MPa and at different states of physical ageing

Physical Ageing Continued

When modelling the creep data using the creep compliance function $D(t)$ it was seen that the only parameter to change in each curve is the mean relaxation time t_0 .

The variation of mean relaxation time t_0 is shown in the figure below



Variation of mean relaxation times t_0 for DP460 with ageing time t_e after curing

This can be represented by the following equation

$$t_0 = B t_e^\mu \quad (3b)$$

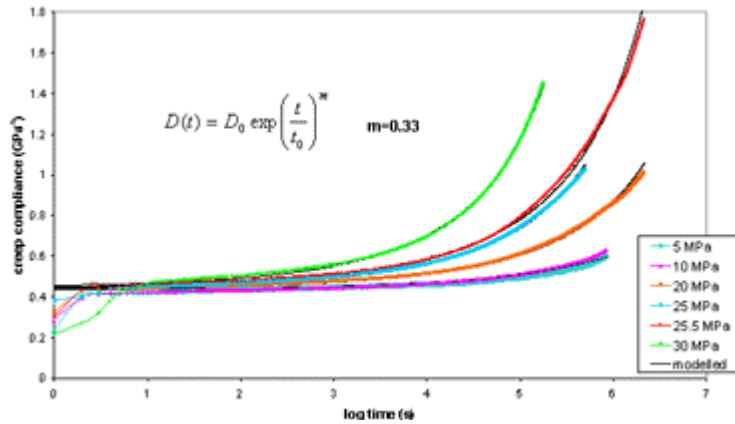
where, for DP460, $\mu=0.87$, and $B=21.9s^{0.13}$

The equation shows that changes in t_0 with time become less as the physical age of the adhesive increases.

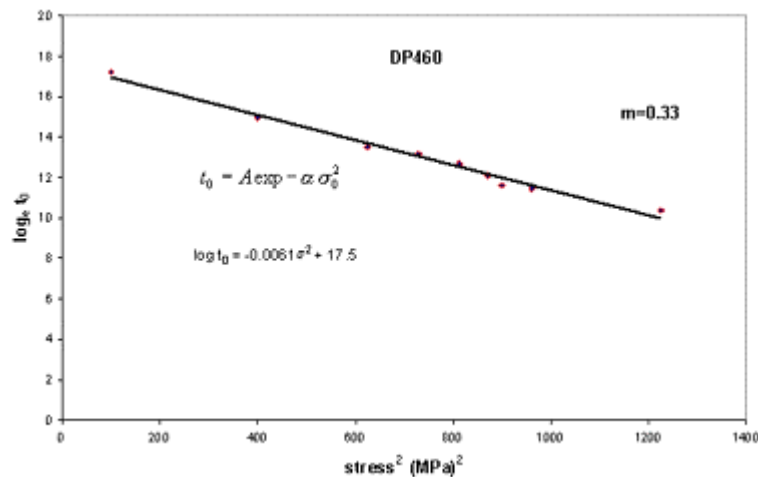
Within this work

- Characterisation of creep behaviour was carried out on specimens that were about 120 days old.
- Duration of these tests was generally around 10 days or less.
- Over this time period, changes in t_0 due to physical ageing will be small so the effects of physical ageing can be neglected in the analysis of creep behaviour.

[BACK](#)



Creep compliance curves for DP460 at different levels of stress



Variation of the mean relaxation time t_0 for DP460 with creep stress σ_0

Non-Linear Creep

The figure on the left shows **Creep compliance curves** for the adhesive DP460 measured under different levels of stress σ_0 .

At short creep times, there is a small dependence of the compliance on stress which is consistent with slight curvature in tensile stress/strain curves obtained from constant displacement rate tests at speeds of typically 10 mm/min. This non-linear behaviour is observed to increase significantly with time under load, the limiting stress for linear behaviour being near or below 10 MPa. The effect of stresses above this level is to give a significant reduction in the mean relaxation time t_0 of the creep process and to, thereby, shift curves to shorter times. This can be demonstrated by obtaining best fitting curves to the data shown using the following equation:

$$D(t) = \frac{\varepsilon(t)}{\sigma_0} = D_0 \exp\left(\frac{t}{t_0}\right)^m \quad (4a)$$

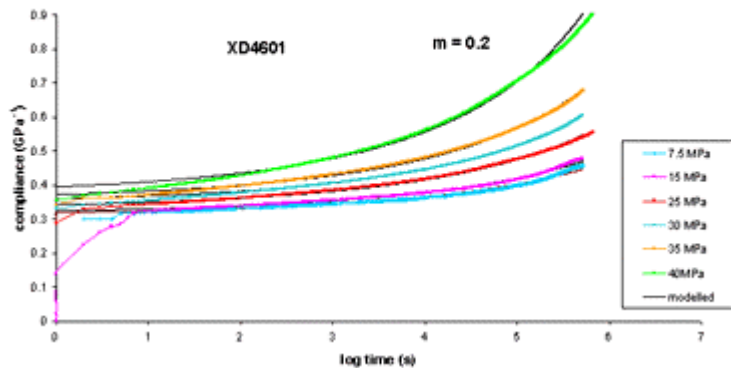
The continuous curves in the figure have been obtained with constant values for $D_0 = 0.44 \text{ GPa}^{-1}$ and $m = 0.33$ and selecting values for t_0 that decrease with increasing stress

The variation of t_0 with σ_0 can be described with satisfactory accuracy by the empirical relationship

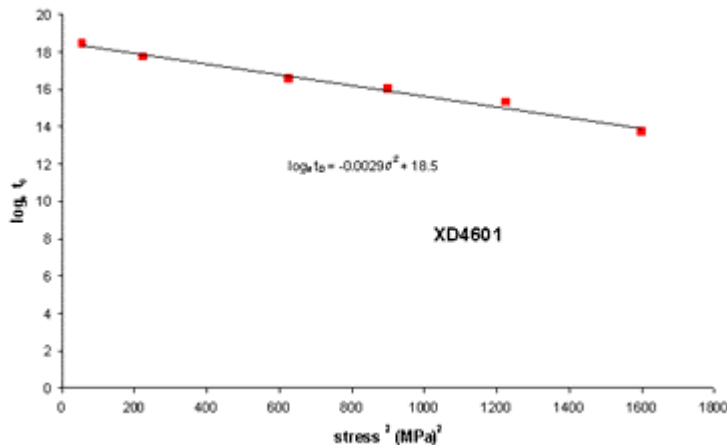
$$t_0 = A \exp -\alpha \sigma_0^2 \quad (4b)$$

as demonstrated by the data for DP460 in the lower left figure. The parameters A and α in this equation can be derived from this figure.

[Non linear creep continued.....](#)



Creep compliance curves for XD4601 at different levels of stress



Variation of the mean relaxation time t_0 for XD4601 with creep stress σ_0

Non-Linear Creep Continued

Creep compliance curves showing the **non-linear creep behaviour** of the adhesive XD4601 under **uniaxial tension** are shown in the top left figure.

The variation of the **mean relaxation time** t_0 for these curves with tensile stress σ_0 is shown in the lower left figure. This follows the same relationship equation as seen with the adhesive DP460.

Values for the parameters in the non-linear creep model represented by the equations

$$D(t) = \frac{\varepsilon(t)}{\sigma_0} = D_0 \exp\left(\frac{t}{t_0}\right)^m \quad \text{and} \quad t_0 = A \exp -\alpha \sigma_0^2$$

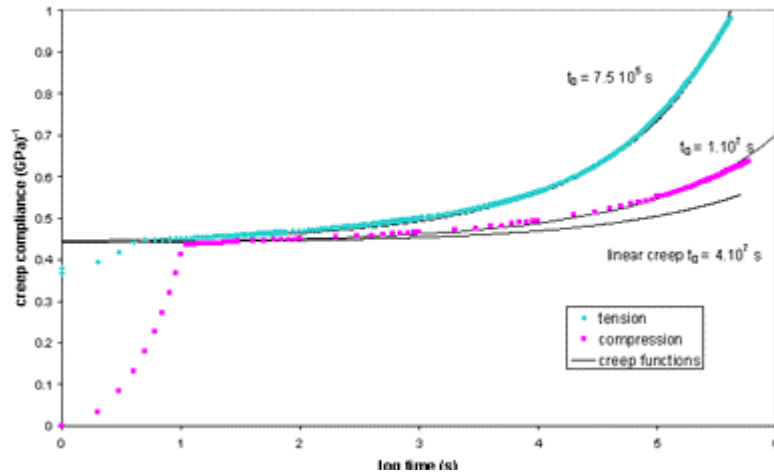
are listed in the table below.

	DP460	XD4601
D_0 (GPa ⁻¹)	0.44	0.34
m	0.33	0.2
A (s)	4.10	10.8
α (MPa ⁻²)	0.0061	0.0029
λ	1.7	

It should be noted that, although creep behaviour can be modelled to satisfactory accuracy using constant values for the model parameters above, small dependencies of D_0 on stress and of t_0 , and hence A and α , on the physical age of the adhesive are evident in experimental data.

[BACK](#)

Creep Under Multiaxial Stresses



Experimental creep data under tension and compression obtained at a stress of 25 MPa. These have been modelled using different relaxation times t_0 . Also shown for comparison is the predicted curve for a low stress where tensile and compressive behaviour is expected to be the same

Under the stress $\sigma_c = 25$ MPa, the results above show that t_0 for the compressive test is 1.10^7 s .

The equations

$$D(t) = \frac{\varepsilon(t)}{\sigma_0} = D_0 \exp\left(\frac{t}{t_0}\right)^m \quad (5a) \quad \text{and} \quad t_0 = A \exp -\alpha \sigma_0^2 \quad (5b)$$

describe creep behaviour under a uniaxial tensile stress.

Modifications to the model are proposed next that will enable creep behaviour to be described under an arbitrary stress state.

The figure (left) compares creep compliance curves for DP460 obtained under uniaxial tensile and compressive stresses of 25 MPa

At low stresses where creep behaviour is linear, compliance curves in tension and compression are expected to be the same. Under the higher stress of 25 MPa where behaviour is non-linear, the results show that the reduction in relaxation time t_0 is less under compression than under tension and hence that it is not only the magnitude of the stress that influences t_0 but the stress state also. The results indicate that the stress in the equation for t_0 should be replaced by an effective stress that is a function of both the shear and hydrostatic components of the creep stress.

[Creep Under Multiaxial Stresses Continued.....](#)

Creep Under Multiaxial Stresses Continued

The simplest function to consider is

$$\bar{\sigma} = \frac{(\lambda+1)}{2\lambda} \sigma_e + \frac{3(\lambda-1)}{2\lambda} \sigma_m \quad (5c)$$

σ_e is the effective shear stress given, in terms of principal components of the applied creep stress, by

$$\sigma_e = \left[\frac{1}{2}(\sigma_1 - \sigma_2)^2 + (\sigma_2 - \sigma_3)^2 + (\sigma_1 - \sigma_3)^2 \right]^{1/2} \quad (5d)$$

σ_m is the hydrostatic component of the creep stress given by

$$\sigma_m = \frac{1}{3}(\sigma_1 + \sigma_2 + \sigma_3) \quad (5e)$$

Combining Equations (5b) and (5c) gives

$$t_o = A \exp -\alpha \bar{\sigma}^2 \quad (5f)$$

Under a tensile creep stress σ_o , $\sigma_e = \sigma_o$ and $\sigma_m = \sigma_o/3$. Under a compressive creep stress σ_c , $\sigma_e = \sigma_c$ and $\sigma_m = -\sigma_c/3$. so, from Equation (5c),

$$\bar{\sigma} = \frac{1}{\lambda} \sigma_c$$

Using the value for t_o ($=1.10^7$ s) from the compressive test at a stress of $\sigma_c = 25$ MPa is the stress, in Equation (5F) gives $\lambda = 1.7$.

[BACK](#)

Implementation of the Creep Model in a Finite Element Analysis

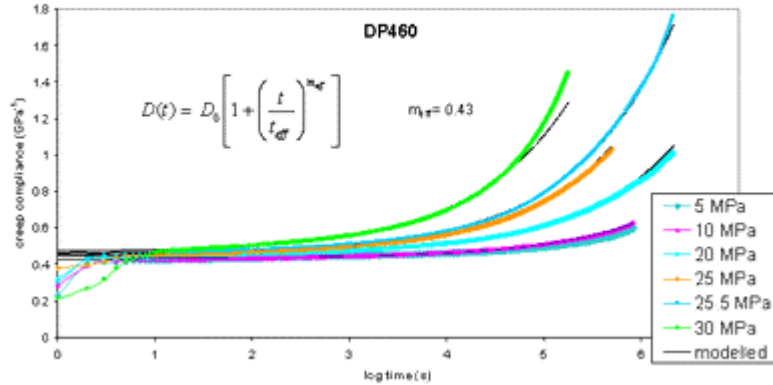
In order to predict stress and strain distributions in an adhesive joint under long-term loading, it is necessary to implement the creep model in a finite element system. The most rigorous method to achieve this is through the development of software for a user-defined materials model (UMAT) for application with the solver in a finite element system. Time limitations in the project have prevented the use of this approach for the work reported here, and so methods for carrying out approximate analyses are considered next.

The use of available non-linear creep models in the finite element system ABAQUS is explored for describing the type of creep behaviour observed in toughened adhesives. These models have been developed for creep in metals at high temperatures and are shown to be unsatisfactory for adhesives.

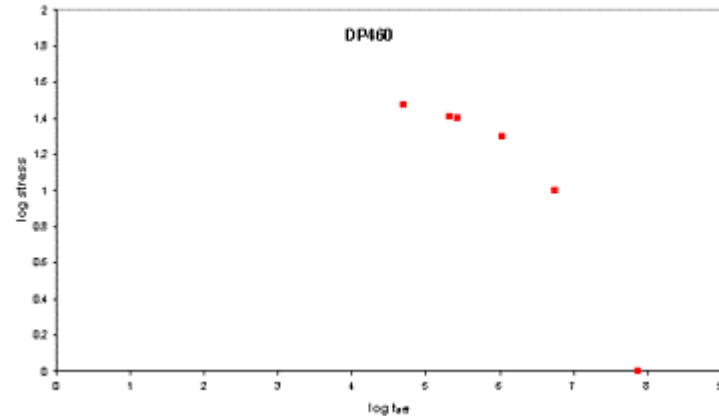
The use of a generalised model for time-dependent plasticity in ABAQUS is interpreted by means of a user-defined subroutine to represent the equations developed to model non-linear viscoelasticity of adhesives.

The use of isochronous stress/strain data in an elastic-plastic analysis is also explored to enable calculations to be carried out of stresses and strains in the adhesive at some specified time. This analysis uses data (isochronous) corresponding to the specified time under a constant load, but the analysis is unable to account for any evolution of stress and strain distributions with time under load by virtue of the time-dependent deformation behaviour of the adhesive.

Applicability of Available Models in Abaqus



Creep compliance data for DP460 modelled using a power law function in time



Plot of log stress against log relaxation time for a power law model demonstrating the unsuitability of Equation (6a) for modelling creep in adhesives.

A creep strain function in ABAQUS that is commonly used to model non-linear creep in metals at elevated temperatures takes the form

$$\varepsilon(t) = \varepsilon_0 + C \sigma_e^n t^{m_{eff}} \quad (6a)$$

where C, n and m_{eff} are material parameters.

This equation relates the time-dependence under creep to a power law in time. The creep compliance curves below can be described with reasonable accuracy using a power law as shown in the top left figure.

The data in this figure have been modelled using the Equation

$$D(t) = D_0 \left[1 + \left(\frac{t}{t_{eff}} \right)^{m_{eff}} \right] \quad (6b)$$

Note, the parameters m_{eff} and t_{eff} will be numerically different from m and t_0 in [Equation \(2c\)](#) in the creep section.

Under a uniaxial tensile creep stress of σ_0 , Equation (6a) becomes

$$D(t) = D_0 + C \sigma_0^{n-1} t^{m_{eff}} \quad (6c)$$

This can be identified with Equation (6b) if

$$\frac{D_0}{t_{eff}^{m_{eff}}} = C \sigma_0^{n-1} \quad (6d)$$

Thus if Equation (6a) is to be applicable to adhesives, a plot of $\log t_{eff}$ vs $\log \sigma_0$ should be linear. This plot for the adhesive DP460 is shown in the lower left figure.

It is clear that these results cannot be approximated by a linear plot, and we can conclude that the creep law in Equation (6a) is not applicable to adhesives.

Implementation of the Creep Model in Abaqus

A generalised creep function in ABAQUS arising from flow by rate-dependent plasticity takes the form

$$\dot{\epsilon}_{ij}(t) = \dot{\epsilon}_s \left(\frac{\partial \sigma_e}{\partial \sigma_{ij}} \right) + \dot{\epsilon}_{sw} \delta_{ij} \quad (7a)$$

This expression can be derived from the flow law in a model for deformation by plasticity where the flow potential has contributions from the shear and hydrostatic stress given by the linear Drucker-Prager model.

$$F = \sigma_e + \mu \sigma_m \quad (7b)$$

where μ is the flow parameter. The terms $\dot{\epsilon}_s$ and $\dot{\epsilon}_{sw}$ can then be associated with contributions to the creep strain rate arising from shear and dilatational (swelling) flow processes.

With reference to Equation (7a) it can be shown that

$$\frac{\partial \sigma_e}{\partial \sigma_{ij}} = \frac{3}{2\sigma_e} (\sigma_{ij} - \sigma_m \delta_{ij}) \quad (7c)$$

Substituting this into Equation (7a) gives

$$\dot{\epsilon}_{ij}(t) = \dot{\epsilon}_s \frac{3\sigma_{ij}}{2\sigma_e} + \left(\dot{\epsilon}_{sw} - \frac{3\sigma_m}{2\sigma_e} \right) \delta_{ij} \quad (7d)$$

The creep function for adhesives,

$$\epsilon(t) = \frac{\sigma_o}{E_o} + \sigma_o \sum_{i=1}^n \frac{1}{E_i} \left(1 - \exp - \left(\frac{t}{\tau_i} \right) \right) \quad (7e)$$

can be generalised to describe multiaxial creep and takes a form similar to Equation (7d), thus

$$\dot{\epsilon}_{ij}(t) = \left((1+\nu) D_o \sigma_{ij} - 3\nu D_o \sigma_m \delta_{ij} \right) \frac{m t^{m-1}}{t_o^m} \exp \left(\frac{t}{t_o} \right)^m \quad (7f)$$

where ν is Poisson's ratio assumed to be independent of time, and t_o is given by

$$t_o = A \exp - \alpha \bar{\sigma}^2 \quad (7g)$$

This can be identified with Equation (7d) if

$$\dot{\epsilon}_s = \frac{2\sigma_e}{3} (1+\nu) D_o \cdot \frac{m}{t_o^m} t^{m-1} \exp \left(\frac{t}{t_o} \right)^m \quad (7h)$$

and

$$\dot{\epsilon}_{sw} = \frac{\sigma_m m}{t_o^m} (1-2\nu) D_o t^{m-1} \exp \left(\frac{t}{t_o} \right)^m \quad (7i)$$

where t_o is a function of σ_e and σ_m given by Equations (7g) and

$$\bar{\sigma} = \frac{(\lambda+1)}{2\lambda} \sigma_e + \frac{3(\lambda-1)}{2\lambda} \sigma_m \quad (7j)$$

The model parameters in these equations have been determined experimentally and have been shown [previously](#). Through Equations (7h) and (7i), a model for non-linear viscoelasticity has been associated with a model for time-dependent plasticity. Coding for a user subroutine has been written so that Equations (7h) and (7i) can be implemented in equation (7a) in ABAQUS for the solution of creep analyses by finite element methods.

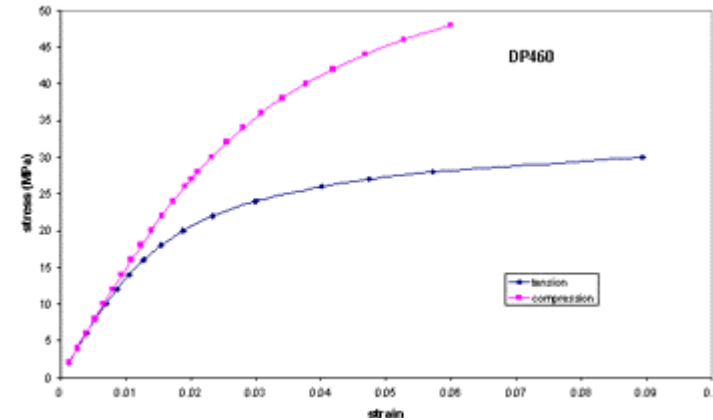
Isochronous Stress/Strain Data

The non-linear creep behaviour of adhesives can be displayed as a series of plots of tensile stress against tensile strain values corresponding to different times under load. These are isochronous curves and can be constructed for arbitrary values of stress using the model equations

$$D(t) = \frac{\varepsilon(t)}{\sigma_o} = D_o \exp\left(\frac{t}{t_o}\right)^m \quad (8a) \quad \text{and} \quad t_o = A \exp - \alpha \sigma_o^2 \quad (8b)$$

which give

$$\varepsilon(t) = \sigma_o D_o \exp\left(\frac{t}{(A \exp - \alpha \sigma_o^2)}\right)^m \quad (8c)$$



Isochronous stress/strain curves for DP460 derived using the creep model at a constant time under load of 10^6 seconds

Using values for the model parameters given [previously](#), Equation (8c) can be used to construct the tensile stress/strain curve shown in the top right figure for DP460 at a time under load of $t = 10^6$ s. Isochronous curves corresponding to loading under uniaxial compression can be calculated by combining Equations (8a) and

$$t_o = A \exp - \alpha \bar{\sigma}^2 \quad (8d)$$

to give

$$\varepsilon_c(t) = \sigma_c D_o \exp\left(\frac{t}{(A \exp - \alpha \bar{\sigma}^2)}\right)^m \quad (8e)$$

where ε_c and σ_c are strains and stresses obtained under a compressive creep stress. The compression curve in the figure above was calculated using Equation (8e).

[Isochronous Data Continued.....](#)

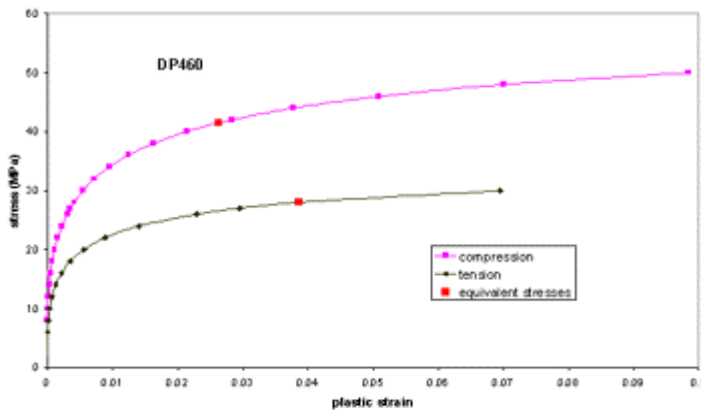
Isochronous Stress/Strain Data

If these data are to be used in an elastic-plastic analysis, it is necessary to present the results [above](#) as hardening curves of stress against the plastic component of strain ϵ^p . These values are derived from the tensile stress and strain values in the figure above using

$$\epsilon^p = \epsilon - \frac{\sigma_o}{E} \quad (8f)$$

where E is Young's modulus appropriate to a loading time of 10^6 s. An analogous equation relates plastic and total strains in a compressive test. A value for E = 1510 MPa was obtained from the linear, small strain region of the curves in the figure above. Hardening data derived using Equation (8f) are shown in the figure below.

The difference between the tensile and compression curves in the figure below demonstrates that non-linear deformation under long-term loading is very sensitive to the hydrostatic component of stress. In an elastic-plastic analysis of this non-linear behaviour, this sensitivity to hydrostatic stress can be included through the use of a model, such as the linear Drucker-Prager model, with a yield criterion that is sensitive to hydrostatic stress. In order to carry out a finite element analysis of a lap joint using isochronous data, the plastic strain hardening behaviour of the adhesive is defined by the tensile hardening curve. The compression curve is then used to derive the hydrostatic stress sensitivity parameter $\mu = \tan \beta$ in the linear Drucker-Prager model. A value for the parameter μ has been calculated from values for the tensile and compressive stresses, σ_o and σ_c respectively, at the same equivalent plastic strain in the figure below using



Stress/plastic strain curves derived from the data in [figure](#) above

$$\mu = \tan \beta = \frac{3(\sigma_c - \sigma_o)}{\sigma_c + \sigma_o} \quad (8g)$$

Equivalent plastic creep strains ϵ^p and ϵ_c^p in tension and compression are related by the equation

$$\sigma_o \epsilon^p = \sigma_c \epsilon_c^p \quad (8h)$$

By way of illustration, one pair of equivalent stresses is shown in the figure, derived using Equation (27). Values for μ obtained from Equations, (8g) and (8h) increase slowly with plastic strain and reach a value of 0.6 at plastic strains of around 0.1. This variation of μ with plastic strain and the associated uncertainty with the derivation of a value for μ illustrates that any attempt to model non-linear creep in adhesives by an elastic-plastic analysis is only approximate.

[BACK](#)

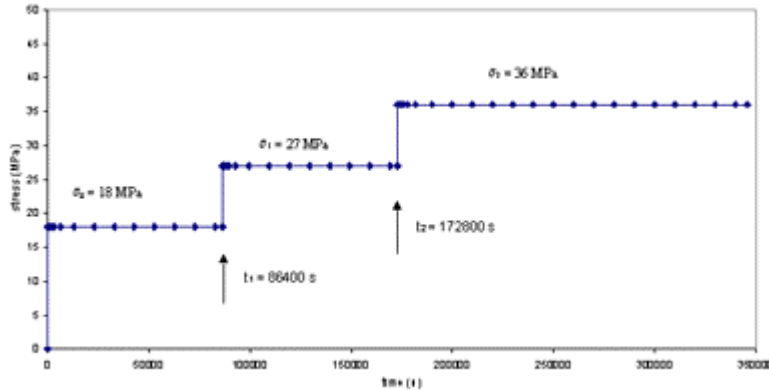
FE Analysis of a Lap Joint Specimen Under Creep Loading

In order to undertake a simple evaluation of the validity of the model developed within the project and the associated subroutine code, predictions have been made of the creep strain produced in a tensile specimen by step increases in the uniaxial tensile stress applied to the specimen.

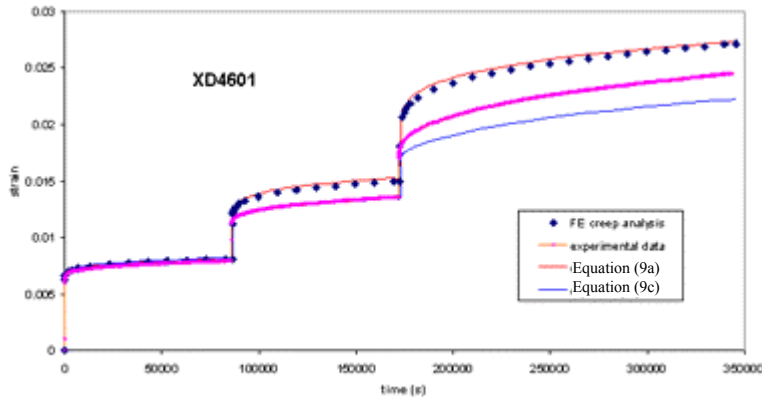
Calculations of stress and strain distributions in the adhesive layer have been carried out using the creep model. Results are shown at loading times of 10s and 10^6 s to demonstrate the evolution of stress and strain distributions with time under load. This analysis is considered to be the more rigorous than the above evaluation.

These results are compared with calculations made using an elastic-plastic model with isochronous hardening data derived using the creep model at 10s and 10^6 s times under load. Two separate analyses are carried out for each time scale, and, as noted earlier, in each analysis the time-dependent behaviour of the adhesive is ignored.

Creep of a Tensile Specimen Under Step Loading



Stress history for creep test and analyses on adhesive XD4601 under step increases in stress



Comparison of creep strains in XD4601 measured under the stress history shown in the figure above with strains calculated using the creep model expressed as time-dependent plasticity in ABAQUS.

The stress history is shown in the figure on the left and this was applied to the adhesive XD4601. Predicted strains using a finite element analysis with a single element representing the gauge region in the tensile specimen are compared with measured values in the lower figure.

It can be seen that the analysis predicts the strain history accurately for the initial stress application only. Significant errors are introduced in strain predictions after the application of each additional step in stress. The reason for this is presumably associated with the procedure used by the FE analysis to generate and superpose calculated strains following each application of additional stress. Thus at times $t > t_2$ corresponding to the application of the second additional stress σ_2 , the analysis appears to use the following expression to calculate the time-dependent strain.

$$\begin{aligned} \varepsilon(t) = & D_o \sigma_o \exp \left(\left(\frac{t_1}{t_o} \right)^m + \left(\frac{t_2 - t_1}{t_o} \right)^m + \left(\frac{t - t_2}{t_o} \right)^m \right) \\ & + D_o (\sigma_1 - \sigma_o) \exp \left(\left(\frac{t_2 - t_1}{t_{o1}} \right)^m + \left(\frac{t - t_2}{t_{o1}} \right)^m \right) \\ & + D_o (\sigma_2 - \sigma_1) \exp \left(\frac{t - t_2}{t_{o2}} \right)^m \quad t > t_2 \end{aligned} \tag{9a}$$

where t_o , t_{o1} and t_{o2} are the relaxation times under stresses σ_o , σ_1 and σ_2 , respectively and are given by

$$t_o = A \exp -\alpha \sigma_o^2 \tag{9b}$$

[Step Loading continued...](#)

Creep of a Tensile Specimen Under Step Loading Continued

It can be seen that this expression does not include any changes to the **relaxation time** for the strain contributions from the stress σ_o on application of the additional stresses σ_1 and σ_2 nor for the strain contribution from the stress σ_1 on application of the stress σ_2 .

An alternative expression Equation (29) allows the relaxation times to change corresponding to the stress level for the appropriate time interval.

$$\begin{aligned} \varepsilon(t) = & D_o \sigma_o \exp \left(\frac{t_1}{t_o} + \frac{t_2 - t_1}{t_{o1}} + \frac{t - t_2}{t_{o2}} \right)^m \\ & + D_o (\sigma_1 - \sigma_o) \exp \left(\frac{t_2 - t_1}{t_{o1}} + \frac{t - t_2}{t_{o2}} \right)^m \\ & + D_o (\sigma_2 - \sigma_1) \exp \left(\frac{t - t_2}{t_{o2}} \right)^m \quad t > t_2 \end{aligned} \quad (9c)$$

The formulation of the superposition of each strain contribution is also different in Equation (9c) from that in Equation (9a)

Although the strain prediction given by Equation (9c) is closer to experimental values (see figure above), there is still a significant departure following the application of the second increment in stress corresponding to a total stress of 36 MPa. Closer examination suggests that this is due to a temporary reduction in the relaxation time value t_{o2} below that given by Equation (9b). This interpretation is consistent with other creep studies under intermittent load and is the subject of further research work.

[BACK](#)

Creep Analysis of a Lap Joint Specimen

Despite the apparent shortcomings in the implementation of the creep model in ABAQUS, as seen in the step loading analysis, a creep analysis has been carried out using the model to determine the evolution of stress and strain distributions with time under load in a lap joint of the adhesive DP460.

The geometry and dimensions of the joint and the element mesh used in the analysis are shown on the right.

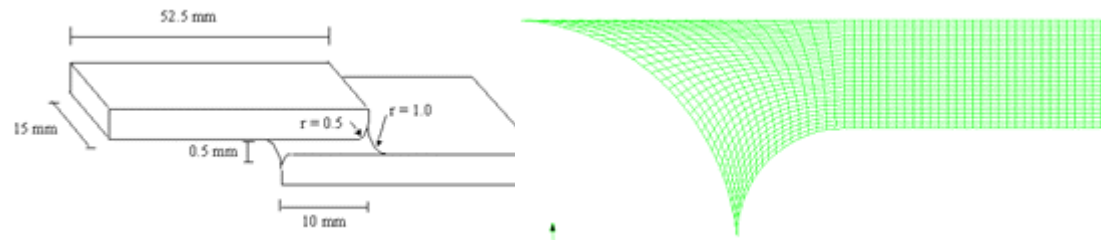
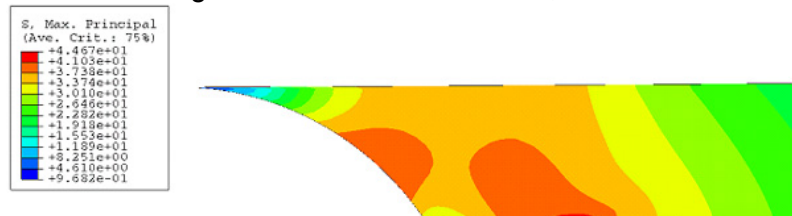


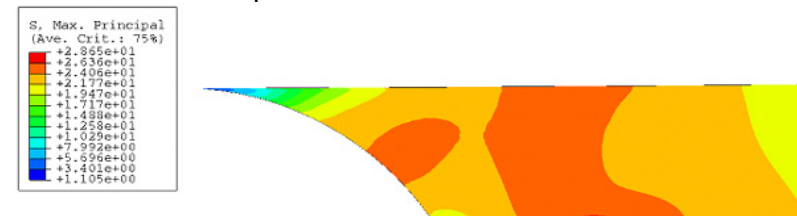
Diagram of the lap joint specimen and the mesh used for the fillet region of the adhesive

The analysis considers a load of 2300N applied to the lap joint for a duration of 10^6 s. Changes in the distribution of the maximum principal stress near the ends of the adhesive layer after 10s and 10^6 s under load are shown in the figures below. These results show a reduction in the level of stress in the adhesive in the region of stress concentration, which is attributable to the non-linear creep behaviour of the adhesive.



Peak stress 44.67 MPa

10 s



Peak stress 28.65 MPa

10^6 s

Lap Joint
ODB: LapJointCreep_2300.odb ABAQUS/Standard 6.3-1 Tue Mar 30 15:55:32 EST 2004
Step: Step-2, Step 2: Creep for 1 million seconds
Increment 171, Step Time = 8.758
Primary Var: S, Max. Principal
Deformed Var: U Deformation Scale Factor: +1.000e+00

Lap Joint
ODB: LapJointCreep_2300.odb ABAQUS/Standard 6.3-1 Tue Mar 30 15:55:32 EST 2004
Step: Step-2, Step 2: Creep for 1 million seconds
Increment 611, Step Time = 1.00000e+06
Primary Var: S, Max. Principal
Deformed Var: U Deformation Scale Factor: +1.000e+00

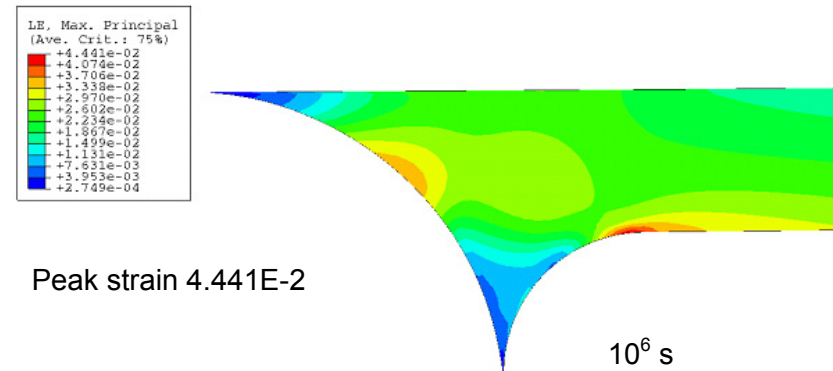
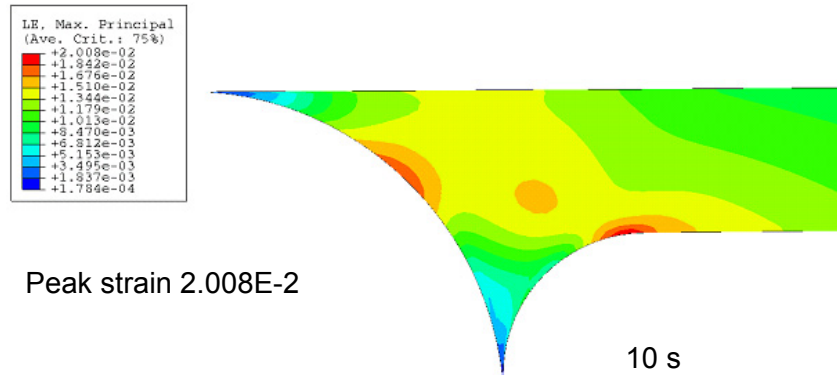
Contours of maximum principal stress in the lap joint after 10 s and 10^6 s under a load of 2300N predicted using the implementation of the creep model in ABAQUS.

[Lap joint analysis continued....](#)

Creep Analysis of a Lap Joint Specimen Continued

In contrast, the figures below show the evolution of the maximum principal strain in the same region of the adhesive.

The strain is seen to increase significantly with time especially in the region of strain concentration.



Lap Joint
ODB: LapJointCreep_2300.odb ABAQUS/Standard 6.3-1 Tue Mar 30 15:55:32 EST 2004
Step: Step-2, Step 2: Creep for 1 million seconds
Increment 171, Step Time = 8.75E
Primary Var: LE, Max. Principal
Deformed Var: U Deformation Scale Factor: +1.000e+00

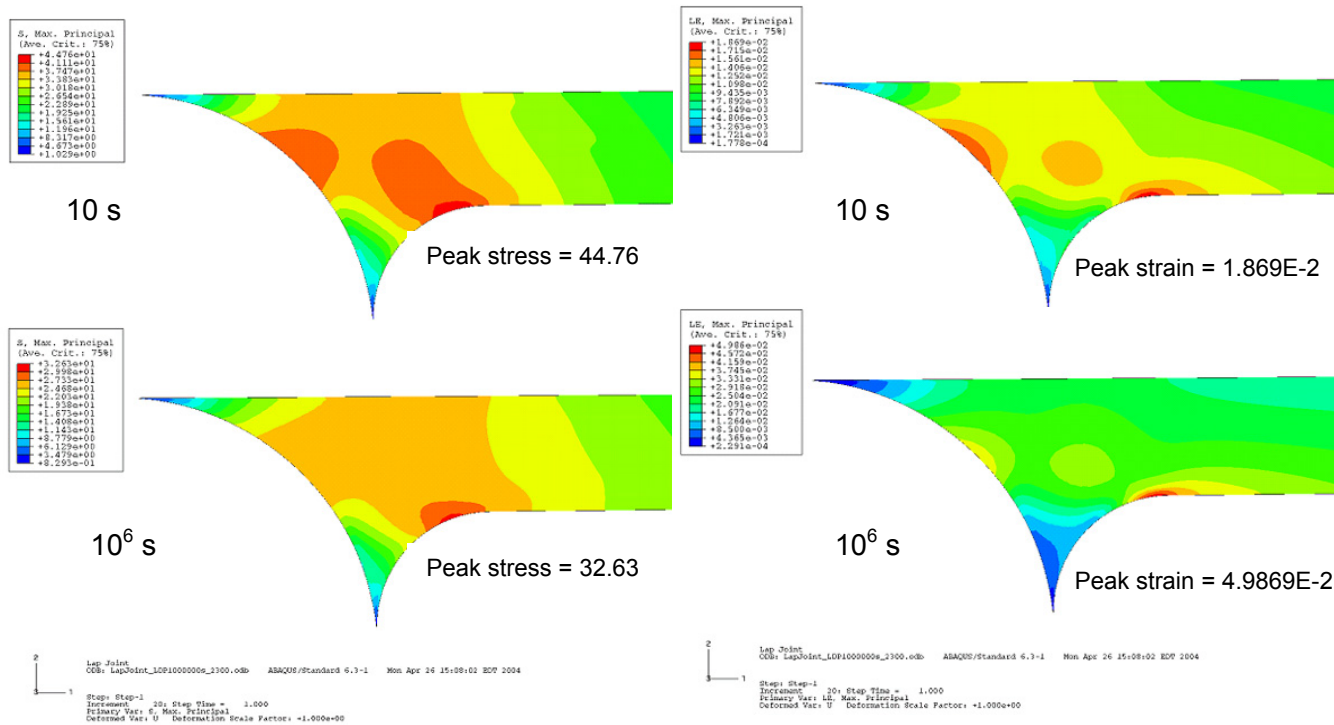
Lap Joint
ODB: LapJointCreep_2300.odb ABAQUS/Standard 6.3-1 Tue Mar 30 15:55:32 EST 2004
Step: Step-2, Step 2: Creep for 1 million seconds
Increment 63, Step Time = 1.0000E+06
Primary Var: LE, Max. Principal
Deformed Var: U Deformation Scale Factor: +1.000e+00

Contours of maximum principal strain in the lap joint after 10 s and 10⁶s under a load of 2300N predicted using the implementation of the creep model in ABAQUS.

[BACK](#)

Application of an Elastic-Plastic Model with Isochronous Data

The figures below show predictions of stress and strain distributions for times of 10s and 10⁶s under load obtained using [isochronous data](#) with an elastic-plastic analysis, analogous to the figures in the [previous](#) section.



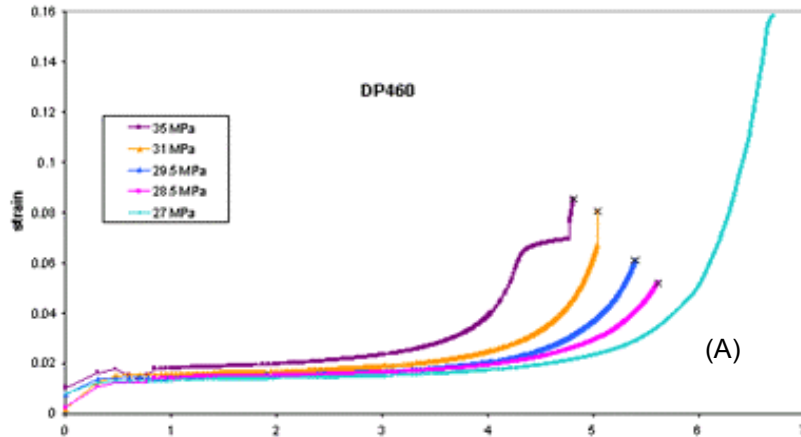
Contours of maximum principal stress in the lap joint after 10 s and 10⁶s under a load of 2300N predicted using an elastic-plastic model with isochronous data.

Contours of maximum principal strain in the lap joint after 10 s and 10⁶s under a load of 2300N predicted using an elastic-plastic model with isochronous data.

Since time-dependent behaviour is not considered in an analysis using isochronous data, two separate analyses were carried out with hardening data appropriate to each time under load. These hardening curves were derived from the creep functions in a previous section on [isochronous data](#).

These calculations gave values for Young's modulus of 2200 MPa and 1510 MPa, respectively, for the 10s and 10⁶s times under load. Values for Poisson's ratio = 0.41 and for the hydrostatic stress sensitivity parameter $\mu = 0.6$ were assumed to be independent of time. The contour maps in the figures show stresses decreasing and strains increasing with time under load as obtained with the creep analyses but the levels of stress and strain are different as would be expected for an approximate analysis.

Long-Term Failure Under Creep Loading



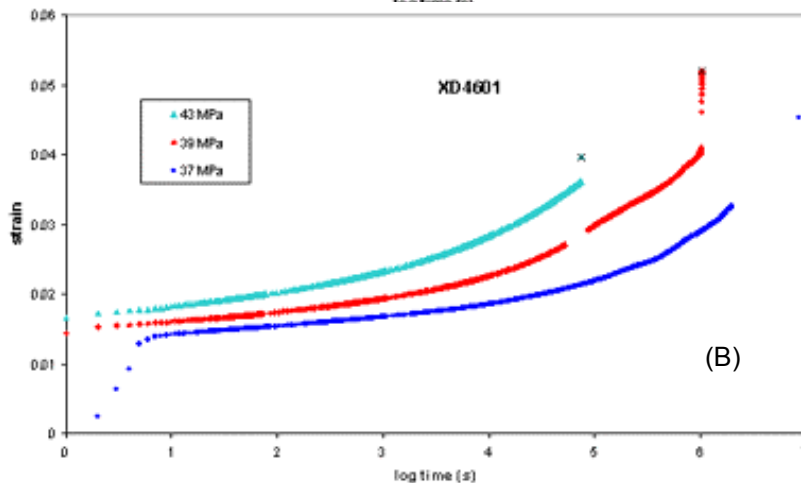
The figures on the left show the results of creep tests on bulk specimens at elevated stresses leading in most cases to rupture of the specimen. In all tests where failure was obtained, an air bubble was observed in the fracture surface. These are presumably the sites of fracture initiation arising from raised stress and strain levels in the vicinity of the bubbles.

Just prior to failure in some of the tests, there is a rapid increase in strain. The fall off in the creep deformation observed near the end of the test at 35 MPa is an artefact of this test and arose because the deformation mechanism of the creep machine reached its limit of travel. The test was continued after the limit was adjusted. The specimens in the tests at 27 MPa in figure labelled (A) and at 37 MPa in figure labelled (B) did not fail within the timescale of the tests.

Although these results are not sufficiently comprehensive to enable conclusions to be drawn regarding a viable criterion for failure of tough adhesives under long-term loading, they indicate that a criterion based on a critical level of a component of strain deserves further study.

Whilst the results show failure at different levels of strain, this can be explained by the stress and strain concentrating effect of air bubbles of different size and location in each specimen. The observation that some specimens in the figures shown are able to sustain high strains without failure (comparable with strain levels in short-term tests under monotonic loading) suggests that there are no bubbles of significant size in these specimens.

The magnitude and the state of strain around a bubble at the instant of failure could be estimated using the creep model developed in this project in conjunction with a finite element analysis that took account of the size and location of the bubble in each specimen. Although not attempted here because of time constraints, such analyses should be carried out as part of the future project on long-term failure of adhesives. A



Strain against log time under load for the adhesives (A) DP460 and (B) XD4601 at different stress levels. The symbol x marks the instant of failure in those tests where failure was observed.

creep analysis would capture the evolution of strain with time under load in a zone of cavitated material around a bubble. A critical strain failure criterion would then be consistent with a failure mechanism involving the growth and coalescence of cavities in this zone to some critical level necessary for failure.

Further Reading

1. [The Use of Finite Element Methods for Design with Adhesives](#),
G Dean and L Crocker, NPL Measurement Good Practice Guide No 48 (2001).
2. Prediction of deformation and Failure of Rubber-Toughened Adhesive Joints,
G Dean, L Crocker, B Read and L Wright, International Journal of Adhesion and Adhesives, Vol 24, Iss 4 (2004) pp 295-306.
3. ISO 3167, Plastics - Multipurpose test specimens
4. Physical Ageing in Amorphous Polymers and Other Materials,
L C Struik, Elsevier, Amsterdam (1978).

[Home](#)

[Introduction](#)

[Materials](#)

[Creep model for Toughened Adhesives](#)

[Linear Creep](#)

[Spring and Dashpot](#)

[Empirical relationship for creep compliance](#)

[Physical ageing](#)

[Non-linear Creep](#)

[Creep under Multiaxial Stress States](#)

[Implementation of the Creep Model in a Finite Element Analysis](#)

[Applicability of Available Models in Abaqus](#)

[Implementation of the creep model in Abaqus](#)

[Isochronous Stress/Strain Data](#)

[FEA of a Lap Joint Specimen](#)

[Creep of a Tensile Specimen Under Step Loading](#)

[Creep analysis of a Lap Joint Specimen](#)

[Application of an Elastic-Plastic Model using Isochronous data](#)

[Long-Term Failure under Creep Loading](#)

[Further Reading](#)